

The bright-end of the luminosity function at $z \sim 9$ [★]

N. Laporte^{1,2}, R. Pelló^{1,2}, M. Hayes^{1,2}, D. Schaerer^{5,2}, F. Boone^{1,2}, J. Richard⁴, J.F. Le Borgne^{1,2}, J.P. Kneib³, and F. Combes⁶

¹ Université de Toulouse; UPS-OMP; IRAP; Toulouse, France

² CNRS; IRAP; 14, avenue Edouard Belin, F-31400 Toulouse, France

e-mail: nicolas.laporte@irap.omp.eu, roser@irap.omp.eu, matthew.hayes@irap.omp.eu, frederic.boone@irap.omp.eu

³ Laboratoire d'Astrophysique de Marseille, CNRS - Université Aix-Marseille, 38 rue Frédéric Joliot-Curie, 13388 Marseille Cedex 13, France

e-mail: jean-paul.kneib@oamp.fr

⁴ Centre de Recherche Astrophysique de Lyon, University Lyon 1, 9 Avenue Charles André, 69561 Saint Genis Laval, France

e-mail: johan.richard@univ-lyon1.fr

⁵ Observatoire de Genève, Université de Genève, 51 Ch. des Maillettes, 1290 Versoix, Switzerland

e-mail: Daniel.Schaerer@unige.ch

⁶ LERMA, Observatoire de Paris and CNRS, 61 Avenue de l'Observatoire, 75014 Paris, France

e-mail: Francoise.Combes@obspm.fr

Received ; accepted

Abstract

Context. We report new constraints on the galaxy luminosity function at $z \sim 9$ based on observations carried out with ESO/VLT FORS2, HAWK-I and X-Shooter around the lensing cluster A2667, as part of our project aimed at selecting $z \sim 7$ -10 candidates accessible to spectroscopy. Only one J - dropout source was selected in this field fulfilling the color and magnitude criteria. This source was recently confirmed as a mid- z interloper based on X-Shooter spectroscopy.

Aims. The depth and the area covered by our survey are well suited to set strong constraints on the bright-end of the galaxy luminosity function and hence on the star formation history at very high redshift.

Methods. The non-detection of reliable J - dropout sources over the ~ 36 arcmin² field of view towards A2667 was used to carefully determine the lens-corrected effective volume and the corresponding upper-limit on the density of sources.

Results. The strongest limit is obtained for $\Phi(M_{1500} = -21.4 \pm 0.50) < 6.70 \times 10^{-6} \text{Mpc}^{-3} \text{mag}^{-1}$ at $z \sim 9$. A maximum-likelihood fit of the luminosity function using all available data points including the present new result yields $M^* > -19.7$ with fixed $\alpha = -1.74$ and $\Phi^* = 1.10 \times 10^{-3} \text{Mpc}^{-3}$. The corresponding star formation rate density should be $\rho_{SFR} < 5.97 \times 10^{-3} M_{\odot} \text{yr}^{-1} \text{Mpc}^3$ at $z \sim 9$. These results are in good agreement with the most recent estimates already published in this range of redshift and for this luminosity domain.

Conclusions. This new result confirms the decrease in the density of luminous galaxies at very high-redshift, hence providing strong constraints for the design of future surveys aiming to explore the very high-redshift Universe.

Key words. surveys – galaxies: high-redshift – cosmology: dark ages, reionization, first stars

1. Introduction

Understanding the formation and evolution of the first galaxies is one of the major topics of modern astronomy. Since a dozen years, many projects and instruments have been developed to push the boundaries of the observed Universe, such as the Hubble Ultra Deep Field (Beckwith et al. 2003) for example. The role played by the first luminous objects in the Universe during the cosmic reionization is still unclear. One way to explore the first epochs is to constrain the number density of galaxies along the cosmic time, and thus establish the Star Formation History (SFH) which represents the evolution of the Star Formation Rate density (SFRd) over the cosmic time. Two complementary approaches could be adopted to further constrain the luminosity function : large blank fields to select the brightest sources, and lensing clusters used as gravitational telescopes to select the faintest ones. Our group has conducted an

observing program combining these two approaches aimed at selecting $z \sim 7$ -10 candidates accessible to spectroscopy, namely the WIRCAM Ultra Deep Survey (WUDS) at CFHT on the CFHTLS-D3 Groth Strip field (Pello et al., to be submitted), and a lensing survey (Laporte et al. 2011, hereafter L11), which is central to this letter.

The galaxy Luminosity Function (LF) is relatively well constrained up to $z \sim 6$. Beyond this limit however the contamination by low- z interlopers becomes more severe because a majority of samples are only supported by photometric considerations, and therefore the results at these redshifts could be seriously affected by contamination (Boone et al. 2011). The only way to get rid of this problem is to spectroscopically confirm, if not all, at least a substantial fraction of sources in a given sample, a performance beyond the capabilities of present-day facilities. Only the brightest samples, including highly magnified sources, could be presently confirmed. Fortunately, the intermediate-to-bright accessible domain ($M_{UV} \sim -20.5$ to -22) is also the most sensitive region of the LF, where most of the evolution is currently observed as a function of redshift (e.g. Bouwens et al.

[★] Based on observations collected at The European Southern Observatory, Paranal, Chile, as part of the ESO 082.A-0163 and 087.A-0118

2010). However, at $z \sim 7-8$ the LF started to be set with recent observations from ground based or space observatories (such as Oesch et al. 2012, McLure et al. 2011, Castellano et al. 2010). Some attempts have been tried up to $z \sim 10$ but without spectroscopic confirmation (Bouwens et al. 2011a).

Deep images of the lensing cluster A2667 were obtained with ESO/VLT FORS 2 and HAWK-I in I , z , Y , J , H and Ks bands. All details regarding these observations and data reduction can be found in L11. IRAC data between 3.6 and $8\mu\text{m}$, and MIPS $24\mu\text{m}$ were also included in the analysis when available (Spitzer Space Telescope, Werner et al. 2004, Fazio et al. 2004, Rieke et al. 2004). Based on these data, 10 photometric candidates at $z \sim 7-10$ were selected based on the usual dropout technique. Among them, only one candidate, J1, is consistent with the $z \sim 9$ J -drop selection criteria, with observed $m_H = 25.21 \pm 0.08$ and a modest magnification factor $\mu = 1.3$. Despite an excellent fit of the photometric SED at high- z , the reliability of this source was already considered as dubious by L11 given the detection of a faint compact counterpart on the HST F850LP/ACS image, with $z_{850} = 27.39 \pm 0.18$. J1 was recently confirmed as a $z = 2.082$ interloper based on the detection of 5 emission lines ($[\text{OIII}]\lambda 5007, 4959, H\alpha, H\beta$ and $\text{Ly}\alpha$) with ESO/VLT X-Shooter spectroscopy (see Hayes et al. 2012, submitted, for more details).

In this letter we report on new constraints on the LF at $z \sim 9$ based on the non-detection of reliable J -dropout candidates over the field of view towards the lensing cluster A2667. The largest magnification regimes cannot be addressed with a single cluster because the effective surfaces/volumes explored in this domain are too small to retrieve significant results. Therefore, this study is limited to the low to moderate magnification regime, where this pilot study provides the most interesting results on the LF as compared to previous studies, in particular blank-field surveys. In Sect. 2 we introduce the method used to constrain the bright-end of the LF at $z \sim 9$, in particular to determine the lens-corrected effective volume and the corresponding upper-limit on the density of sources. The constraints derived on the SFH at $z \sim 9$ are presented in Sect. 3. A brief discussion and conclusions are given in Sect. 4. Throughout this paper, a concordance cosmology is adopted, with $\Omega_\Lambda = 0.7$, $\Omega_m = 0.3$ and $H_0 = 70 \text{ km s}^{-1} \text{ Mpc}^{-1}$. All magnitudes are given in the AB system (Oke & Gunn 1983).

2. The luminosity function at $z \sim 9$

The non-detection of reliable J -dropout candidates over the field of view toward A2667 is used in this Section to carefully determine the lens-corrected effective volume at $z \sim 9$ and the corresponding upper-limits on the density of sources. In the following, we only consider the field of view corresponding to the surface covered with more than 75% of the total exposure time in all filters. A mask was also applied to remove all the noisy regions within and around galaxies from the subsequent analysis. The region masked is only $\sim 12\%$ of the total area, but it reaches a maximum of $\sim 30\%$ in the cluster core, within the 1 arcmin^2 centered on the cD galaxy. The final effective area is $\sim 36 \text{ arcmin}^2$.

The selection criteria adopted by L11 for $8.5 \lesssim z \lesssim 9.5$ candidates require a detection above 5σ level within a $1.3''$ diameter aperture in H , i.e. $H < 26.22$, and the usual color selection as follows: $J - H > 0.76$, $H - Ks < 0.5$, and $J - H > 1.3 \times (H - Ks) + 0.76$. In practice, the depth in the J -band limits the reliability of the J -dropout selection to $H < 26.0$, corresponding to a completeness level higher than 90%. Absolute

Table 1. Upper limits for the luminosity function at $z = 8.5-9.5$, for different magnifications regimes and UV luminosities.

μ	μ	μ	Surface	Volume	$H <$	M_{1500}	$\Phi \times 10^{-6}$
mean	min	max	arcmin ²	$\times 10^4 \text{ Mpc}^3$	mag		$\text{Mpc}^{-3} \cdot \text{mag}^{-1}$
1.04	1.02	1.05	32.55	5.7602	26.02	-21.35	6.70
1.12	1.05	1.2	27.01	4.7798	26.06	-21.31	8.07
1.35	1.2	1.5	9.47	1.6758	26.22	-21.15	23.0
2.40	1.5	3.3	2.31	0.4088	26.93	-20.44	94.4

magnitudes in the $\sim 1500\text{\AA}$ domain (M_{1500}) are derived from H -band magnitudes assuming a flat spectrum.

As compared to blank fields, data obtained in gravitational-lensing fields need to be corrected for both magnification and dilution effects. A magnification factor μ introduces an enhancement on the observed luminosity, depending on the redshift of the source and the location of the image on the sky, without modifying the color-selection window. Dilution reduces the effective surface covered by the survey, in such a way that a pixel affected by a magnification factor μ has an effective area reduced by the same factor on the corresponding source plane. We have used the lensing model for A2667 originally obtained by Covone et al. (2006) to compute the magnification map at $z \sim 9$ using the public software *Lenstool*¹, including the MCMC optimization method of Jullo et al. (2007). We explicitly compute the effective surface probed by the survey through a pixel-to-pixel integration of the magnification map, after masking the pixels lying in the object's mask, as explained above. The effective surface is 32.55 arcmin^2 , corresponding to a covolume of 57602.5 Mpc^3 between $z \sim 8.5$ and 9.5 .

The effective limiting magnitude for the detection of $z \sim 9$ candidates, however, depends on the magnification factor μ . To take this effect into account when deriving upper-limits on the density of sources, we have considered different magnification regimes, with effective surface/covolume decreasing with increasing μ . Table 1 summarizes these results and provides the non-detection constraints obtained on the LF. Areas, volumes and limiting magnitudes quoted in this table are effective lens-corrected ones. Given the low to moderate magnification regimes explored in this study, uncertainties in the effective surveyed volumes due to lensing-modeling uncertainties are considered negligible (see also Maizy et al. 2010 for details). The strongest limit is obtained for $\Phi(M_{1500} = -21.4 \pm 0.50) < 6.70 \times 10^{-6} \text{ Mpc}^{-3}$ at 68% confidence level assuming Poissonian statistics. Figure 1 displays the independent data points on the LF, together with previous results from the literature. We also computed points from Zheng et al. (2012), for comparison purpose, using MC approach taking into account the probability distribution in redshift (Bolzonella et al. 2002) and considering two different values for the magnification: $\mu \sim 15$, as reported by the authors, and $\mu \sim 8$, as obtained from the MACS1149+22 model by Smith et al. (2009).

We have adopted the Schechter parametrization of the LF (Schechter 1976):

$$\Phi(M_{1500}) = \Phi^* \frac{\ln(10)}{2.5} \left(10^{-0.4(M-M^*)} \right)^{\alpha+1} \exp\left(-10^{-0.4(M-M^*)} \right) \quad (1)$$

to set constraints on M^* using a χ^2 minimization, assuming a fixed $\alpha = -1.74$ (Bouwens et al. 2008). Our two independent limits in Φ at $M_{1500} = -21.35$ and -20.44 have been combined to the available upper limits from the HUDF and GOODS fields at the

¹ <http://www.oamp.fr/cosmology/lenstool>

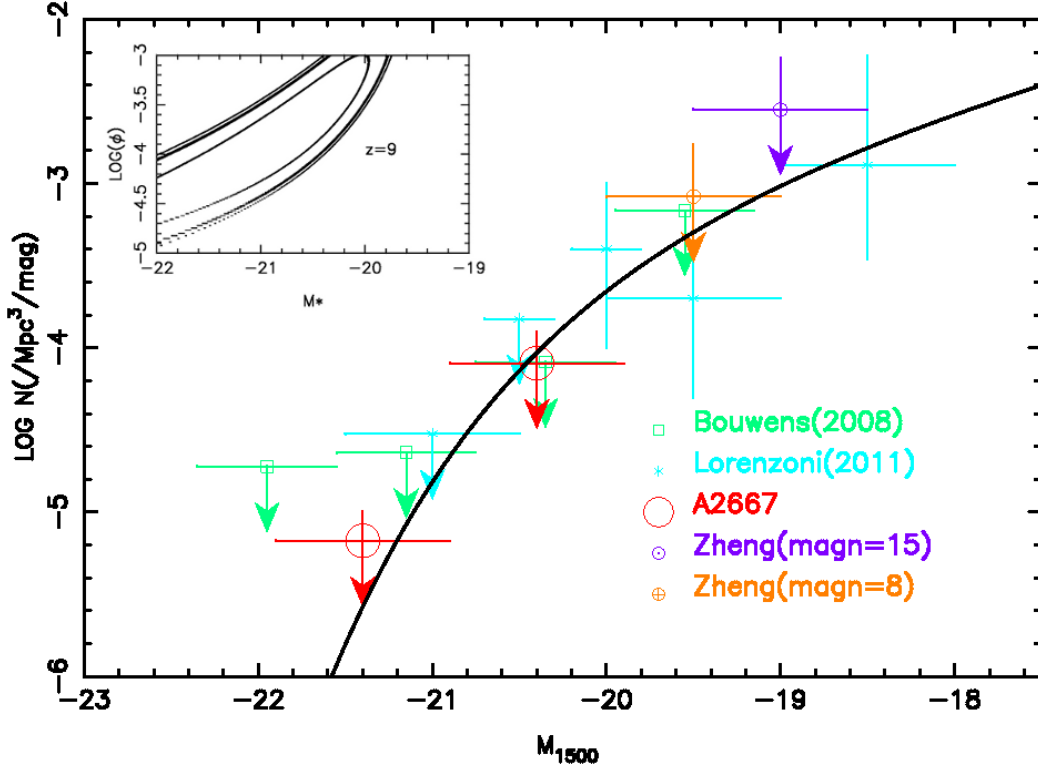


Figure 1. Luminosity function at $z \sim 9$ showing the upper limits resulting from the absence of J -dropout sources in our HAWK-I survey (red dots including cosmic variance), upper limit from Bouwens et al. (2008) found in the HUDF and GOODS field of view (green dot). We also plot points obtained from the $z \sim 9$ candidate of Zheng et al. (2012) considering a magnification factor of $\mu \sim 15$, and the amplification factor $\mu \sim 8$ obtained using the model by Smith et al. (2009) for MACS1149+22 (error bars take into account the cosmic variance computed from Trenti & Stiavelli (2008)) and points from Lorenzoni et al. (2011) at $z \sim 8-9$. The last data set is only displayed for comparison purposes; it was not used for the computation of the LF at $z \sim 9$ given the difference in the redshift domain. The dark line displays the Schechter function using $M^* = -19.7$, $\alpha = -1.74$ and $\Phi^* = 1.10 \times 10^{-3} \text{Mpc}^{-3} \text{mag}^{-1}$. The small panel displays the likelihood contours for the 1, 2 and 3 σ confidence regions for a fixed $\alpha = -1.74$.

same redshift domain than in Bouwens et al. (2008). As shown in Fig. 1, given the degeneracy between Φ^* and M^* , and the small number of available data points at $z \sim 9$, we can only derive a limit for Φ^* when assuming M^* or vice-versa. It has been shown that Φ^* seems not evolve significantly from $z \sim 4$ to 9, whereas M^* clearly decreases over $z \sim 4-8$ (e.g. Bouwens et al. (2011b)). Assuming this no-evolution, we have used a fixed $\Phi^* = 1.10 \times 10^{-3} \text{Mpc}^{-3}$ and we obtain $M^* > -19.7$. This result is also consistent with previous findings (Bouwens et al. (2008)).

3. The star formation history up to $z \sim 9$

The SFH could be explored through the evolution of the SFRd over the cosmic time. Using the shape of the LF found in the previous section, we are now able to constrain the SFRd at $z \sim 9$. This density is deduced from the UV density produced by Lyman Break galaxies and usually defined by :

$$\rho_{UV} = \int_{0.05L_{z=3}^*}^{\infty} L_{1500} \Phi(L_{1500}) dL_{1500} \quad (2)$$

where $L_{z=3}^* = 1.33 \times 10^{41} \text{erg s}^{-1} \text{\AA}^{-1}$ and $\Phi(L_{1500})$ is the UV LF. The lower integration bound was chosen in order to facilitate the comparison with previous studies (see Sect. 4). The conversion between UV density and SFRd is done using the Kennicutt (1998) relation given by :

$$\rho_{SFR} (\text{M}_{\odot} \cdot \text{yr}^{-1} \cdot \text{Mpc}^{-3}) = 1.40 \cdot 10^{-28} \times \rho_{UV} (\text{erg} \cdot \text{s}^{-1} \cdot \text{Mpc}^{-3} \cdot \text{\AA}^{-1}) \quad (3)$$

As a result, the SFRd limit at $z \sim 9$ is found, using $M^* = -19.7$, to be $\rho_{SFR} < 5.97 \times 10^{-3} \text{M}_{\odot} \text{yr}^{-1} \text{Mpc}^{-3}$. Fig. 2 shows the evolution of the SFRd versus cosmic time including results already published over a large range in redshift. For consistency, all points in this figure up to $z \sim 7$ have been corrected for dust extinction (at $z \geq 8$ we considered that dust attenuation is negligible). A parameterization as a function of redshift has been derived based on the expression for dust extinction given by Schiminovich et al. (2005) as a function of the UV slope, the evolution of which as a function of redshift is taken from Schiminovich et al. (2005) for $z \leq 3.5$, and extended from $z \sim 3.5$ up to 7 according to Bouwens et al. (2011b). The expression² given by Cole et al. (2001) is used to fit the SFH, in order to compare the above value of ρ_{SFR} with the trend observed between $z \sim 3$ and 8. The best-fit parameters of the Cole function are found to be $a=0.0$, $b=0.10$, $c=2.85$ and $d=4.65$. As seen in Fig. 2, our result is compatible with the evolution observed below $z \sim 8$, and it is also consistent with the SFRd limit published at $z \sim 10$ by Bouwens et al. (2011a).

4. Discussion and Conclusions

Over the $\sim 36 \text{arcmin}^2$ field of view of our survey around the lensing cluster A2667, only one J -dropout candidate was retained (L11). This source, already considered as a possible interloper

² $\rho_{*} = \frac{a+bz}{1+(\frac{z}{c})^d} \text{h} \quad \text{M}_{\odot} \cdot \text{yr}^{-1} \cdot \text{Mpc}^{-3}$

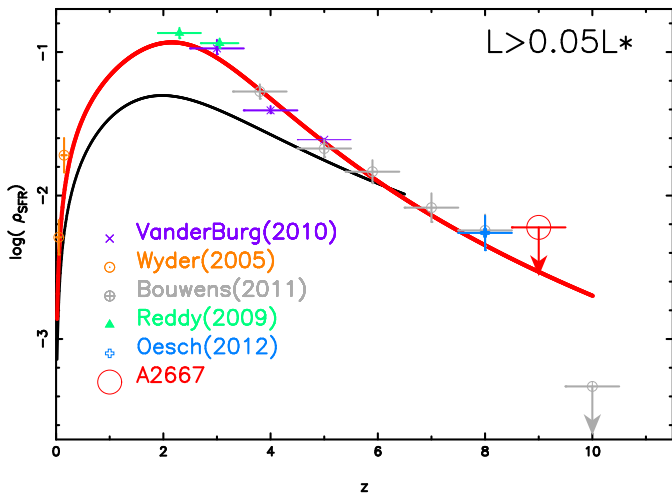


Figure 2. Star formation history including the present result at Wyder et al. (2005), Reddy & Steidel (2009), van der Burg et al. (2010), Oesch et al. (2012)). For consistency, all points in this figure have been corrected for dust reddening (see text). The red line shows the parametrization of the corrected SFH following Cole et al. (2001) (see text) and the dark line displays the evolution of uncorrected SFRd (i.e. without dust extinction correction; the corresponding points are not shown to avoid confusion).

by L11, has been recently confirmed at $z=2.082$ based on the detection of five emission lines with ESO/VLT X-Shooter spectroscopy (see Hayes et al., submitted, for more details). The non-detection of J -dropout candidates in our survey is consistent with previous non-detections reported by Bouwens et al. (2008) in the HDF, HUDF and GOODS fields (4.8, 9.1 and 9.3 arcmin² respectively), with m_H (5σ , 0.6arcsec aperture) typically ranging between ~ 27.6 to 26.6, and also complementary in terms of surface covered and effective depth.

Assuming that there is no reliable $z \sim 9$ candidate in our survey up to $m_H = 26.0 + 2.5 \times \log(\mu)$, we take benefit from the depth and large area covered to set strong constraints on the bright-end of the LF and hence on the SFH at very high redshift by a careful determination of the lens-corrected effective volume and corresponding upper-limits on the density of sources. We have considered different magnification regimes, with effective surface/covolume decreasing with increasing μ . The strongest limit is obtained for $\Phi(M_{1500} = -21.4 \pm 0.50) < 6.70 \times 10^{-6} \text{Mpc}^{-3} \text{mag}^{-1}$ at 68% confidence level assuming Poissonian statistics.

We combined our two independent LF limits at $M_{1500} = -21.35$ and -20.44 with the available upper limits for the HUDF and GOODS fields, extracted from Bouwens et al. (2008), to derive the Schechter parameters for the LF. Assuming a fixed $\alpha = -1.74$ and no-evolution in $\Phi^* = 1.10 \times 10^{-3} \text{Mpc}^{-3}$, we obtain a constrain on $M^* > -19.7$. This result is consistent with previous findings, e.g. Bouwens et al. (2008), Castellano et al. (2010) ($M^*(z \sim 7) \sim -20.24$) and Oesch et al. (2012) ($M^*(z \sim 8) \sim -19.80$). The corresponding SFRd given the previous LF should be $\rho_{SFR} < 5.97 \times 10^{-3} M_{\odot} \text{yr}^{-1} \text{Mpc}^3$ at $z \sim 9$. These results are in good agreement with the most recent estimates already published in this range of redshift and for this luminosity domain, and confirm the decrease in the density of luminous galaxies from $z \sim 6$ to 9, hence providing strong constraints for the design of future surveys aiming to explore the very high-redshift Universe.

Several projects such as CLASH (Postman et al. 2011) or CANDELS (Grogin et al. 2011) are currently ongoing to con-

strain the evolution of galaxies beyond $z \sim 6$. However, all samples highlighted by these projects need to be confirmed by deep spectroscopic observations beyond the limits of current spectrographs. Near-IR spectrographs are also needed to understand the nature of (extreme) mid- z interlopers presently found in such deep surveys. The arrival of multi-object near-IR facilities such as EMIR/GTC (Balcells et al. 2000, Pelló et al. 2011) or KMOS/VLT (Sharples et al. 2006, Sharples et al. 2010) will introduce a substantial progress in this area. Given the results presented in this paper, increasing by a factor of ~ 10 the sample of lensing clusters with deep multi-wavelength photometry over a large field of view, similar to our survey in A2667, is expected to set crucial constraints on the intermediate-to-high luminosity domain at $z \sim 7-10$, and substantially improve the selection of spectroscopic targets. Such a cluster sample will provide a reference frame allowing to connect the results obtained in blank fields with those obtained in the strongest magnification regimes, as shown in this letter.

Acknowledgements. Part of this work was supported by the French CNRS, the French Programme National de Cosmologie et Galaxies (PNCG), as well as by the Swiss National Science Foundation. This work received support from the Agence Nationale de la Recherche bearing the reference ANR-09-BLAN-0234.

References

- Balcells, M., Guzman, R., Patron, J., et al. 2000, in Society of Photo-Optical Instrumentation Engineers (SPIE) Conference Series, Vol. 4008, Society of Photo-Optical Instrumentation Engineers (SPIE) Conference Series, ed. M. Iye & A. F. Moorwood, 797–805
- Beckwith, S. V. W., Caldwell, J., Clampin, M., et al. 2003, in Bulletin of the American Astronomical Society, Vol. 35, American Astronomical Society Meeting Abstracts #202, 723
- Bolzonella, M., Pelló, R., & Maccagni, D. 2002, A&A, 395, 443
- Boone, F., Schaerer, D., Pelló, R., et al. 2011, A&A, 534, A124
- Bouwens, R. J., Illingworth, G. D., Franx, M., & Ford, H. 2008, ApJ, 686, 230
- Bouwens, R. J., Illingworth, G. D., Labbe, I., et al. 2011a, Nature, 469, 504
- Bouwens, R. J., Illingworth, G. D., Oesch, P. A., et al. 2011b, ArXiv e-prints
- Castellano, M., Fontana, A., Paris, D., et al. 2010, A&A, 524, A28
- Cole, S., Norberg, P., Baugh, C. M., et al. 2001, MNRAS, 326, 255
- Covone, G., Kneib, J.-P., Soucail, G., et al. 2006, A&A, 456, 409
- Fazio, G. G., Hora, J. L., Allen, L. E., et al. 2004, ApJS, 154, 10
- Grogin, N. A., Kocevski, D. D., Faber, S. M., et al. 2011, ApJS, 197, 35
- Hayes, M., Laporte, N., Pelló, R., Schaerer, D., & Le Borgne, F. 2012, submitted to MNRAS
- Jullo, E., Kneib, J.-P., Limousin, M., et al. 2007, New Journal of Physics, 9, 447
- Kennicutt, Jr., R. C. 1998, ApJ, 498, 541
- Laporte, N., Pelló, R., Schaerer, D., et al. 2011, (L11)A&A, 531, A74
- Lorenzoni, S., Bunker, A. J., Wilkins, S. M., et al. 2011, MNRAS, 414, 1455
- McLure, R. J., Dunlop, J. S., de Ravel, L., et al. 2011, MNRAS, 418, 2074
- Oesch, P. A., Bouwens, R. J., Illingworth, G. D., et al. 2012, ArXiv e-prints
- Oke, J. B. & Gunn, J. E. 1983, ApJ, 266, 713
- Pelló, R., Garzón, F., Balcells, M., et al. 2011, in SF2A-2011: Proceedings of the Annual meeting of the French Society of Astronomy and Astrophysics, ed. G. Alecian, K. Belkacem, R. Samadi, & D. Valls-Gabaud, 161–167
- Postman, M., Coe, D., Benitez, N., et al. 2011, ArXiv e-prints
- Reddy, N. A. & Steidel, C. C. 2009, ApJ, 692, 778
- Rieke, G. H., Young, E. T., Engelbracht, C. W., et al. 2004, ApJS, 154, 25
- Schechter, P. 1976, ApJ, 203, 297
- Schimionovich, D., Ilbert, O., Arnouts, S., et al. 2005, ApJ, 619, L47
- Sharples, R., Bender, R., Agudo Berbel, A., et al. 2010, in Society of Photo-Optical Instrumentation Engineers (SPIE) Conference Series, Vol. 7735, Society of Photo-Optical Instrumentation Engineers (SPIE) Conference Series
- Sharples, R., Bender, R., Bennett, R., et al. 2006, New A Rev., 50, 370
- Smith, G. P., Ebeling, H., Limousin, M., et al. 2009, ApJ, 707, L163
- Trenti, M. & Stiavelli, M. 2008, ApJ, 676, 767
- van der Burg, R. F. J., Hildebrandt, H., & Erben, T. 2010, A&A, 523, A74
- Werner, M. W., Roellig, T. L., Low, F. J., et al. 2004, ApJS, 154, 1
- Wyder, T. K., Treyer, M. A., Milliard, B., et al. 2005, ApJ, 619, L15
- Zheng, W., Postman, M., Zitrin, A., et al. 2012, ArXiv e-prints